VIP Gas-Phase MRI

DOI: 10.1002/ange.200700830

Para-Hydrogen-Enhanced Hyperpolarized Gas-Phase Magnetic Resonance Imaging**

Louis-S. Bouchard, Kirill V. Kovtunov, Scott R. Burt, M. Sabieh Anwar, Igor V. Koptyug, Renad Z. Sagdeev, and Alexander Pines*

Herein, we demonstrate magnetic resonance imaging (MRI)[1] in the gas phase using para-hydrogen (p-H_2)-induced polarization.[2] A reactant mixture of H_2 enriched in the para spin state and propylene gas is flowed through a reactor cell containing a heterogenized catalyst, Wilkinson's catalyst immobilized on modified silica gel. The hydrogenation product, propane gas, is transferred to the NMR magnet and is spin-polarized as a result of the ALTADENA (adiabatic longitudinal transport and dissociation engenders net alignment) effect.[3] A polarization enhancement factor of 300 relative to thermally polarized gas was observed in 1D ^{1}H NMR spectra. Enhancement was also evident in the magnetic resonance images. This is the first demonstration of imaging a hyperpolarized gaseous product formed in a hydrogenation reaction catalyzed by a supported catalyst. This result may lead to several important applications, including flow-through porous materials,[4,5] gas-phase reaction kinetics and adsorption studies, and MRI in low fields,[6] all using catalyst-free polarized fluids.

Gas-phase MRI suffers from the problem of low sensitivity, which makes it difficult to image void spaces such as those in the lung and in porous materials. This limitation has led to the use of hyperpolarized gases[7,8] such as ^{129}Xe, ^{3}He, and, more recently, ^{83}Kr. Other approaches have used fast-relaxing inert fluorinated gases[9] or higher gas pressures.[10] Hyperpolarized noble gases and polarization instruments are generally expensive.

[*] Dr. L.-S. Bouchard, S. R. Burt, Dr. M. S. Anwar, Prof. A. Pines
Department of Chemistry
University of California
Berkeley and Division of Materials Science
Lawrence Berkeley National Lab
1 Cyclotron Road, Bldg. 11-D64, Berkeley, CA 94720 (USA)
Fax: (+1) 510-486-5744
E-mail: sabieh@berkeley.edu

K. V. Kovtunov, Prof. I. V. Koptyug, Prof. R. Z. Sagdeev
International Tomography Center
3 A Institutskaya St., Novosibirsk 630090 (Russia)

[**] This work was supported by the Director, Office of Science, Office of Basic Energy Sciences, Materials Sciences and Engineering Division, of the U.S. Department of Energy (contract no. DE-AC03-76SF00098) and the CRDF (grant RU-C1-2581-NO-04) and was partially supported by grants from the RFBR (05-03-32472), SB RAS (integration grant no. 11), RAS (5.1.1 and 5.2.3), and the Russian President's Program of Support of the Leading Scientific Schools (grant NSch-4821.2006.3). S.R.B. thanks the U.S. Department of Homeland Security for support through a graduate fellowship, administered by ORISE under the DOE contract number DE-AC05-06OR23100. I.V.K. thanks the Russian Science Support Foundation for financial support.

Another method for producing hyperpolarized fluids is by using para-hydrogen,[2] which has a zero total nuclear spin angular momentum ($I = 0$) and is therefore not detectable in an NMR experiment. Mixtures enriched with one of the spin isomers provide large non-equilibrium nuclear spin order. This enhanced spin order can be converted into an enhanced NMR signal if the enriched ortho-/para-hydrogen mixture participates in a hydrogenation reaction that breaks the symmetry of the original H_2 molecule. If the hydrogenation reaction preserves the spin correlation between the protons, this correlation can be converted into a strong observable nuclear spin polarization.

The method is not limited to protons only, as polarization transfer mechanisms[11] can be employed to polarize other nuclei as well, such as the slowly relaxing ^{13}C. Contrast agents based on p-H_2 polarization have indeed been demonstrated[12] and provide high-quality, angiographic ^{13}C MR images of the blood vessels in animal models. However, these experiments were conducted in the liquid phase and the polarized fluid is contaminated with the homogeneous catalyst, which often poisons the animal. An exception is the work reported by Bhattacharya et al.,[12c] whereby the catalyst was recovered before the polarized fluid was injected into the subject. However, catalyst recovery is not straightforward for all kinds of catalysts. Furthermore, the lifetime of the polarized state is often short, typically on the order of a few seconds for ^{1}H; thus, elaborate recovery procedures can easily destroy the polarization.

Heterogeneous catalysis avoids these problems. The catalyst can be fixed in place, for example, immobilized on a solid matrix,[13] and thus, produce a stream of polarized, catalyst-free fluid. The catalyst is not used up and can be reused with the next batch of reactants, which saves on cost and eliminates potential problems associated with contamination of the fluid by the catalyst.

We have recently reported[14] the creation and observation of para-hydrogen-induced polarization in heterogeneous hydrogenation reactions. These results verified the preservation of the nuclear spin correlation and also give essential insights into the reaction mechanism: most importantly, that the homogeneous catalyst *does* maintain its reaction mechanism upon immobilization.

Herein, we report the first demonstration of signal enhancement in gas-phase imaging with the use of a supported catalyst. We demonstrate gas-phase proton imaging of the hyperpolarized product resulting from para-hydrogenation of a substrate molecule, in our case, propylene (CH_3–CH=CH_2). The reaction is catalyzed by heterogenized Wilkinson's catalyst supported on modified silica gel ([RhCl-

$(PPh_3)_2PPh_2(CH_2)_2]$–SiO_2) and results in the formation of propane ($CH_3CH_2CH_3$). The p-H_2-derived protons in propane (labeled as H_A and H_B in Scheme 1) preserve their nuclear spin singlet state,[2d,15] $(|\alpha\beta\rangle - |\beta\alpha\rangle)/\sqrt{2}$, characterized by anti-

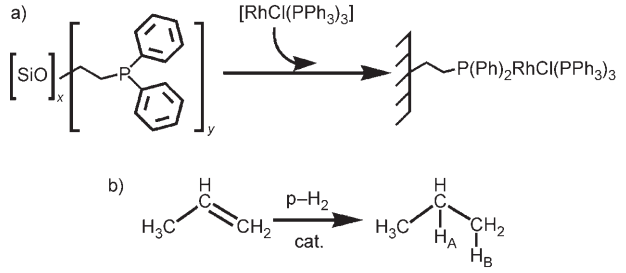

Scheme 1. a) Schematic of the preparation of the supported catalyst used in the study. b) Para-hydrogenation of propylene to form propane gas (the protons from p-H_2 in propane are labeled H_A and H_B).

symmetric spin correlation. The reactant–product mixture is then adiabatically transferred to the high field of the NMR magnet, leading to preferential population of the $|\alpha\beta\rangle$ (or the $|\beta\alpha\rangle$) state, an experimental scheme referred to as ALTADENA.[3] The resulting NMR signal is enhanced compared to what is achievable with thermal population of spin states.

The enhancement is commonly evaluated with respect to the thermal equilibrium state. The signal intensity obtainable from the thermal state depends on the magnetic field strength and temperature and is proportional to $h\gamma B/kT$ (h: Planck's constant; γ: magnetogyric ratio; B: magnetic field; k: Boltzmann's constant; T: temperature). Therefore, even though the p-H_2-derived polarization is field-independent,[15,16] the enhancement *does* depend on the reference field for the thermal state (assuming constant T). For example, for a 10 T field the enhancement can be about 3×10^4, and for the earth's field it can be much bigger ($\approx 6\times10^9$).

The nuclear spin states in the ALTADENA experiment can be characterized in terms of density matrices and product operators.[15–17] Hydrogenation takes place in the catalytic cell that is placed in the earth's magnetic field ($\approx$0.5 G), where the thermal equilibrium spin density matrix is a mixture of the singlet state (S_0) and equal amounts of each of the three triplets (T_0, T_1, and T_{-1}); these states are in fact the eigenstates of the earth's field nuclear spin rotating frame Hamiltonian [Eq. (1)], where J is the scalar coupling constant

$$\mathscr{H}_{\rm low} = 2\pi J\,(I_x S_x + I_y S_y + I_z S_z) \tag{1}$$

between the protons and I and S represent the angular momentum spin operators for the two nuclear spins. In the rotating frame, the Zeeman terms are small in the earth's field and are therefore neglected. This low-field Hamiltonian corresponds to an A_2 spin system.

The singlet and triplet eigenstates are defined as follows:[15a,16] $S_0 = |S_0\rangle\langle S_0|$, $T_0 = |T_0\rangle\langle T_0|$, $T_1 = |T_1\rangle\langle T_1|$, and $T_{-1} = |T_{-1}\rangle\langle T_{-1}|$, where $|S_0\rangle = (|\alpha\beta\rangle - |\beta\alpha\rangle)/\sqrt{2}$, $|T_0\rangle = (|\alpha\beta\rangle + |\beta\alpha\rangle)/\sqrt{2}$, $|T_1\rangle = |\alpha\alpha\rangle$, and $|T_{-1}\rangle = |\beta\beta\rangle$. If the molar fraction of the singlet in the hydrogen mixture is s, the density matrix after hydrogenation will comprise a fraction s of the spin singlet and $1-s$ of a balanced mixture of the three spin triplets [Eq. (2)] and can be expressed in product operator terms as shown in Equation (3).

$$\rho_{\rm low} = s\,S_0 + (1-s)\,(T_0 + T_1 + T_{-1})/3 \tag{2}$$

$$\rho_{\rm low} = \mathbf{1}/4 + (1-4s)/3\,(I_x S_x + I_y S_y + I_z S_z) \tag{3}$$

Clearly, this is a non-equilibrium state. Compared to the thermal equilibrium state [Eq. (4)] ($\varepsilon \approx h\gamma B/kT$), the coefficient of the polarization terms in $\rho_{\rm low}$ lies between -1 and 1, implying enhancement factors of up to about $1/\varepsilon$.

$$\rho_{\rm eq} = \mathbf{1}/4 + \varepsilon\,(I_z + S_z) \tag{4}$$

As propane is adiabatically transferred to the high field of the magnet, the Hamiltonian gradually transforms to its high-field form [Eq. (5)], with f_1 and f_2 corresponding to the magnetic-field-dependent offset frequencies of protons H_A and H_B.

$$\mathscr{H}_{\rm high} = 2\pi\,(f_1 I_z + f_2 S_z + J I_z S_z) \tag{5}$$

This high-field Hamiltonian is accurate under the condition that $|f_1 - f_2| \gg |J|$ and corresponds to an AX spin system. The eigenstates of $\mathscr{H}_{\rm high}$ are $|\alpha\alpha\rangle$, $|\alpha\beta\rangle$, $|\beta\alpha\rangle$, and $|\beta\beta\rangle$.

According to the quantum adiabatic theorem,[18] the overall quantum state must conserve its respective projections onto the instantaneous eigenstates of the transforming Hamiltonian. One can show[3,16] that as the field is adiabatically increased, $|S_0\rangle$ and $|T_0\rangle$ transform into $|\alpha\beta\rangle$ and $|\beta\alpha\rangle$ (or vice versa, depending on the sign of $(f_1-f_2)/J$). This implies that the spin populations in the state $|S_0\rangle$ ($|T_0\rangle$) will be carried over into state $|\alpha\beta\rangle$ ($|\beta\alpha\rangle$). Consequently, in a high field, the spins of H_A and H_B in propane will be in the state described by Equation (6).

$$\begin{aligned}\rho_{\rm high} &= s|\alpha\beta\rangle\langle\alpha\beta| + (1-s)/3\,(|\beta\alpha\rangle\langle\beta\alpha| + |\alpha\alpha\rangle\langle\alpha\alpha| + |\beta\beta\rangle\langle\beta\beta|)\\ &= \mathbf{1}/4 - (1-4s)/6\,I_z + (1-4s)/6\,S_z + (1-4s)/3\,I_z S_z\end{aligned} \tag{6}$$

(For convenience we assume that $|S_0\rangle$ maps into $|\alpha\beta\rangle$ and that $|T_0\rangle$ maps into $|\beta\alpha\rangle$.) However, the polarization in $\rho_{\rm high}$ is still non-observable, therefore the state must be rotated with a radiofrequency pulse with a certain flip angle, θ. From the rotated state, one can deduce the expected multiplet pattern.[16] In our case, the expected spectrum is proportional to that shown in Equation (7), where each term represents the *relative* intensity of the individual lines in the multiplets, with the leftmost two representing the first (I) and the rightmost representing the second spin (S). For example, with a $\theta = \pi/4$ nutation pulse, the expected spectral pattern is proportional to [0.3, 1.7, −1.7, −0.3]. This prediction is in agreement with the experimental observation.

$$\sin\theta\,[(1-\cos\theta),\,(1+\cos\theta),\,(-1-\cos\theta),\,(-1+\cos\theta)] \tag{7}$$

For our experiments, a hydrogen mixture enriched in the para spin state (50% p-H_2) was produced by passing pure

hydrogen gas through a tubular cell that was packed with FeO(OH) and immersed in a Dewar flask containing liquid N_2. The ortho/para ratio was verified by measuring the NMR signal intensities of H_2 in a cell packed with porous alumina (γ-Al_2O_3; the method is detailed elsewhere[14]). An aluminum cylinder was filled with the para-enriched H_2 to 80 psi, and propylene was then added to a total pressure of 100 psi (Scheme 2). Consequently, the volumetric composition in the reactant mixture was 20% propylene, 40% p-H_2, and 40% o-H_2.

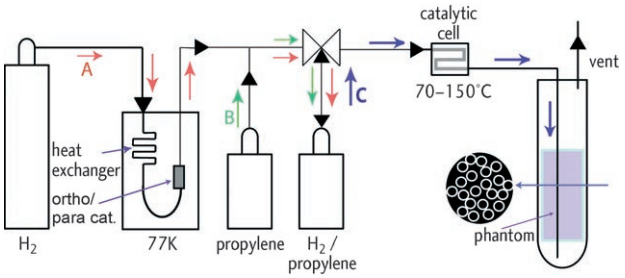

Scheme 2. Flow diagram for the gas-phase experiment. The red arrows (A) represent the flow of the H_2 gas, the green arrows (B) represent the flow of propylene, and the blue arrows (C) depict the flow of the H_2 and propylene mixture. Normal H_2 (25% para) flows through an o/p catalyst, FeO(OH), held at 77 K to produce a stream of 50% para-H_2, which is then stored in the small cylinder, to which propylene is added. This experiment used a sample of 40% ortho-H_2, 40% para-H_2, and 20% propylene with a total pressure of 100 psi. A mixture of propylene and para-enriched H_2 flows into a catalytic cell containing catalyst supported on silica gel and held at 70–150°C. The product, propane, as well as unreacted propylene and H_2 flow into the magnet, resulting in ALTADENA polarization of the propane. The gas flows through a 1/16 inch ($\approx$0.16 cm) capillary to the bottom of the NMR tube and up through a phantom, either a cross shape or a random packing of 1/16 inch ($\approx$0.16 cm) capillaries. A cross section of the latter is shown.

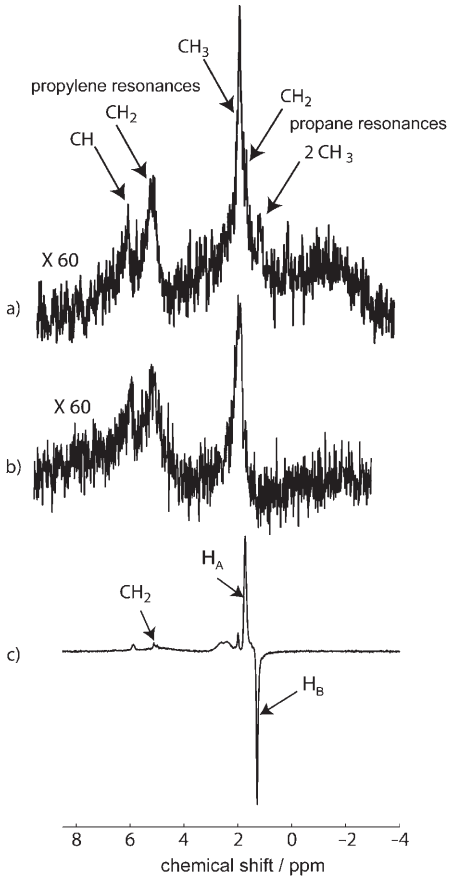

Figure 1. ^{1}H NMR spectra of a) fully relaxed and thermally polarized mixture of propylene and propane acquired 2 min after stopping the flow, b) propylene under flowing conditions, and c) a mixture of propylene and the polarized propane gas under flowing conditions and with heating of the catalyst. The peaks from the p-H_2-derived protons and the CH_2 peak in the unreacted propylene are marked in spectrum (c). Spectra (a) and (b) have been magnified 60 times.

The supported catalyst was prepared[14,19,20] by the addition of an approximately stoichiometric amount of 2-diphenylphosphinoethyl-functionalized silica gel to a solution of Wilkinson's catalyst in toluene (Scheme 1). The solution was stirred overnight, and the catalyst was filtered, washed with toluene, and dried under vacuum at room temperature. All the chemicals used in the synthesis were obtained from Sigma-Aldrich and used as received. All manipulations with the catalyst were performed under nitrogen gas atmosphere.

A sample of the catalyst ($\approx$0.1 g) was packed between plugs of glass wool inside a 15-cm-long section (6 inch) of copper tubing ($d \approx 0.32$ cm (1/8 inch)), bent into an S-shaped catalytic reactor. The reactor (polarizer) was held at a temperature of approximately 150°C. The gas mixture flowed through the catalytic cell and then through Teflon tubing ($d \approx 0.32$ cm (1/8 inch)), which finally transitioned into a Teflon capillary ($d \approx 0.16$ cm (1/16 inch)) ending at the bottom of a 10 mm NMR tube. The tube was placed inside the high field of a vertical bore, 300 MHz NMR magnet (Varian Inc.) equipped with imaging gradient coils. The phantoms were placed near the bottom of the NMR tube and held in the sensitive region of the detector.

The ^{1}H NMR spectra are shown in Figure 1. Figure 1b shows the spectrum of propylene acquired under flowing conditions and before any reaction was performed. The reaction was then carried out by heating the catalytic cell. The emissive and absorptive ALTADENA peaks and the smaller peaks from the unreacted propylene appear in the resulting spectrum (Figure 1c). This latter spectrum was also acquired under flow conditions. The propylene peaks correspond to *partially* relaxed thermal polarization and are much smaller compared to the ALTADENA peaks and serve as an internal intensity reference. In another experiment, the catalytic cell was maintained at high temperature, the gaseous mixture of reactants and product was transferred to the NMR tube, and the flow was stopped. Figure 1a shows the resulting spectrum acquired two minutes after stopping the flow. Owing to the long residence time in the NMR tube, complete thermal equilibration can be assumed; the spectrum illustrates the maximum amount of obtainable thermal polarization. Furthermore, by comparing the signal intensity per proton between propane (product) and propylene (reactant), we estimate the reaction yield to be about 5%. The spectra

acquired in the flowing and stopped-flow conditions are different, reflecting the different pressures and the extent of thermal equilibration achieved during the transit and residence times in the magnet.

Images of gas flowing in the void space surrounding the phantom were acquired using the pure phase-encoding protocol.[1] The pulse sequence consisted of a 45° radio-frequency nutation pulse, tipping ρ_{high} into the observation plane.[17] The detectable terms were then spatially encoded by a 200-μs-long phase-encoding gradient pulse. The free induction decay was subsequently acquired in the absence of any gradient. This sequence was repeated for 21×21 steps of the x and y phase-encoding gradients. The maximum phase-encoding gradient pulse amplitude was 70 G cm^{-1}. The frequency components of interest were then selected for the generation of the image. The field of view was 12 mm × 12 mm, which resulted in an in-plane spatial resolution of 0.57 mm × 0.57 mm. The thickness of the image plane (along the z direction) was 10 mm.

The signal from one of the ALTADENA peaks was integrated to generate the ALTADENA image shown in Figure 2c and e. The signal-to-noise ratio, as measured directly from the magnitude image (average signal in the gas space divided by the standard deviation of noise located at the edges of the field of view), was 150 in the channels of the phantom with the weaker signal and 200 in the channel exhibiting the strongest signal. In Figure 2c, no signal is seen in the 0.16 cm (1/16 inch) capillary because of the higher flow velocity in it. The strongest signal is seen in the channel opposite to the capillary because a higher fraction of the incident gas is deflected by the round bottom of the glass NMR tube into the opposite channel. The total scan time was 8 min, owing to the long recycle delay of 1 s, but could be optimized.

The geometry can be compared to the conventional MRI image, where the void space surrounding the phantom was filled with water (Figure 2a). Also shown in Figure 2b and d is the thermally polarized signal obtained by integrating the CH_2 peaks of the unreacted propylene (also marked in Figure 1b). The resulting image exhibits almost no signal except for a slight zero-frequency artifact. This means that compared to the ALTADENA peaks, the thermal polarization is exceedingly low. As a second phantom, we used a random packing of capillaries mimicking a porous medium. The images reconstructed from the unpolarized propylene and ALTADENA-polarized propane peaks are shown in Figure 2d and e.

The exact amount of polarization enhancement compared to other proton resonances is difficult to obtain directly from these images because of the poor signal in Figure 2b and d. The ALTADENA signal yields image signal-to-noise ratios of 150–200. From the data of Figure 1a, we estimate the reaction yield to be 5% (1/20). The enhancement factor is obtained from the reaction yield and knowledge of the amount of thermal repolarization that is found by comparing the total signal per proton between the stopped-flow and flowing spectra in Figure 1a and b. We estimate that during flowing conditions, the propylene peaks are polarized to only about 50% of their thermal equilibrium value. From the data in

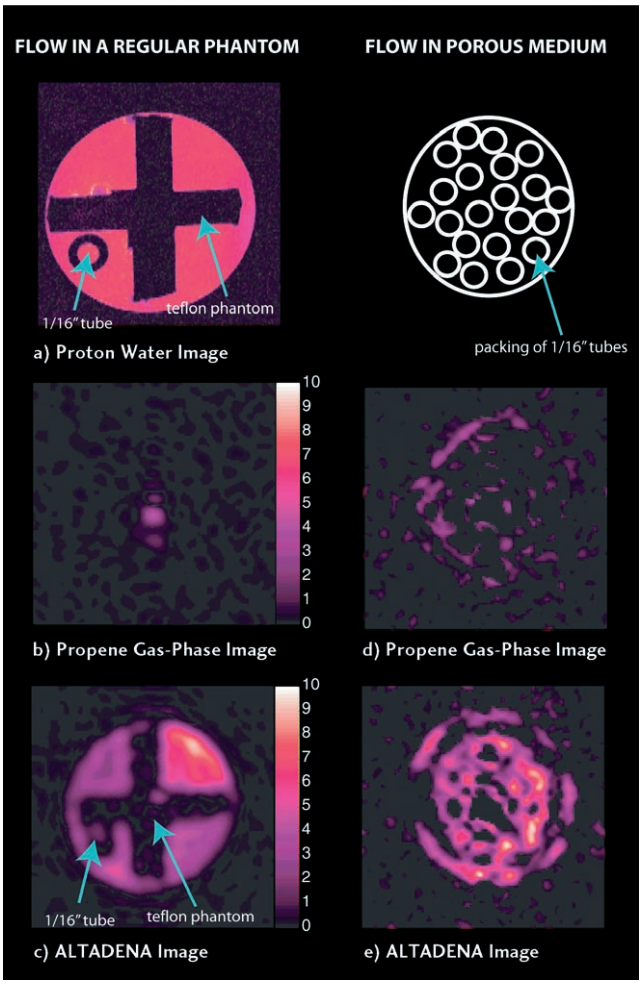

Figure 2. a) High-resolution water proton image for a thin cross-sectional slice through a cross-shaped Teflon phantom. The circle depicts the Teflon tube (0.16 cm or 1/16 inch) which delivers the gas. b) Propylene gas phase image based on the signal intensity from the CH_2 peak. c) ALTADENA image from the propane CH_3 peak. Parts (b) and (c) were reconstructed from the same experiment and are plotted with respect to the same color scale. Images (d) and (e) correspond to a phantom consisting of a random packing of capillaries to demonstrate gas-phase MRI through a porous medium.

Figure 1c, the ratio of peak areas for ALTADENA-enhanced propane protons to thermally polarized propylene protons is about 30:1. The enhancement factor is therefore $30 \times 20 \times 1/2 = 300$, an enhancement of two orders of magnitude relative to the thermally polarized gas.

It is also important to note that these experiments were not optimized. The imaging experiments, for example, could use more efficient pulse sequences, which include shorter recycle times[1] and frequency-selective pulses[22] that excite only the ALTADENA resonances followed by frequency-encoded readouts or even one-shot readouts. Further optimizations to the polarizer could be made by maximizing the surface-to-volume ratio of the supported catalyst bed or by adjusting the flow velocity, temperature, and pressure of the reaction. We note that the enhancement factor of 300 is considerably less than the theoretical ALTADENA enhancement expected from 50% polarized p-H_2. This is due to a

combination of the short T_1 relaxation of propane protons caused by the spin-rotation interaction,[9] the dipolar relaxation in the intermediate dihydride, and relaxation during contact of the polarized product with the porous catalyst support.

A broader range of applications of this heterogeneous reaction would be possible if the gas were condensed into a liquid by cooling following the hydrogenation. Because the singlet state of p-H_2-derived product can be preserved for very long periods of time in the earth's field,[21] the product can be stored prior to its usage. At the time of use, the hydrogenated substrate can be transported to the high magnetic field (ALTADENA effect) or suddenly dephased by a non-adiabatic field to create the incoherent I_zS_z state for subsequent use in low magnetic field environments. It is also possible to transfer polarization to ^{13}C nuclei[11] for lifetime enhancement and then transfer it back to ^1H nuclei for detection. Applications to medical imaging,[23] such as lung imaging, are also possible if issues of gas toxicity can be addressed. A further threefold enhancement (see Equation (3)) in the signal intensity is also achievable by using 100% p-H_2.

In summary, we have illustrated the application of p-H_2-induced polarization with a supported catalyst to magnetic resonance imaging in the gas phase. Situations in which polarization enhancements can be envisaged include microfluidic flow, imaging of lungs and other porous materials, as well as MRI in low magnetic fields.

Received: February 23, 2007
Published online: April 23, 2007

Keywords: ALTADENA · heterogeneous catalysis · magnetic resonance imaging · NMR spectroscopy · para-hydrogen induced polarization

[1] P. Callaghan, *Principles of Nuclear Magnetic Resonance Microscopy*, Oxford University Press, USA, **1994**.
[2] a) C. R. Bowers, D. P. Weitekamp, *Phys. Rev. Lett.* **1986**, *57*, 2645 – 2648; b) J. Natterer, J. Bargon, *Prog. Nucl. Magn. Reson. Spectrosc.* **1997**, *31*, 293 – 315; c) C. R. Bowers, D. P. Weitekamp, *J. Am. Chem. Soc.* **1987**, *109*, 5541 – 5542; d) C. R. Bowers in *Encyclopedia of NMR*, *Advances in NMR*, *Vol. 9* (Eds: D. M. Grant, R. K. Harris), Wiley, Chichester, **2002**, pp. 750 – 770.
[3] M. G. Pravica, D. P. Weitekamp, *Chem. Phys. Lett.* **1988**, *145*, 255 – 258.
[4] R. W. Mair, G. P. Wong, D. Hoffmann, M. D. Hürlimann, S. Patz, L. M. Schwartz, R. L. Walsworth, *Phys. Rev. Lett.* **1999**, *83*, 3324 – 3327.
[5] a) E. Harel, J. Granwehr, J. A. Seeley, A. Pines, *Nat. Mater.* **2006**, *5*, 321 – 327; b) C. Hilty, E. McDonnell, J. Granwehr, S.-I. Han, K. Pierce, A. Pines, *Proc. Natl. Acad. Sci. USA* **2005**, *102*, 14960 – 14963.
[6] a) A. W. Foy, S. Saxena, A. J. Moulé, H.-M. L. Bitter, J. A. Seeley, R. McDermott, J. Clark, A. Pines, *J. Magn. Reson.* **2002**, *157*, 235 – 241.
[7] a) G. E. Pavlovskaya, Z. I. Cleveland, K. F. Stupic, R. J. Basaranabar, T. Meersman, *Proc. Natl. Acad. Sci. USA* **2005**, *102*, 18275 – 18279; b) K. Ruppert, J. F. Mata, J. R. Brookeman, K. D. Hagspiel, J. P. Mugler III, *Magn. Reson. Med.* **2004**, *51*, 676 – 687; c) R. W. Mair, M. I. Hrovat, S. Patz, M. S. Rosen, I. C. Ruset, G. P. Topulos, L. L. Tsai, J. P. Butler, F. W. Hersman, R. L. Walsworth, *Magn. Reson. Med.* **2005**, *53*, 745 – 749; d) E. Brunner, M. Haake, L. Kaiser, A. Pines, J. A. Reimer, *J. Magn. Reson.* **1999**, *138*, 155 – 159.
[8] a) A. Kastler, *J. Phys. Radium* **1950**, *11*, 255; b) B. M. Goodson, *J. Magn. Reson.* **2002**, *155*, 157 – 216.
[9] a) D. O. Kuethe, A. Caprihan, H. M. Gach, I. J. Lowe, E. Fukushima, *J. Appl. Physiol.* **2000**, *88*, 2279 – 2286; b) D. C. Roe, P. M. Kating, P. J. Krusic, B. E. Smart, *Top. Catal.* **1998**, *5*, 133 – 147.
[10] M. J. Lizak, M. S. Conradi, C. G. Fry, *J. Magn. Reson.* **1991**, *95*, 548.
[11] a) D. Blazina, S. B. Duckett, J. P. Dunne, C. Godard, *Dalton Trans.* **2004**, 2601 – 2609; b) H. Jóhannesson, O. Axelsson, M. Karlsson, *C. R. Phys.* **2004**, *5*, 315 – 324; c) S. Aime, R. Gobetto, F. Reineri, D. Canet, *J. Chem. Phys.* **2003**, *119*, 8890 – 8896.
[12] a) K. Golman, O. Axelsson, H. Jóhannesson, S. Månsson, C. Olofsson, J. S. Petersson, *Magn. Reson. Med.* **2001**, *46*, 1 – 5; b) H. Jóhannesson, O. Axelsson, M. Karlsson, *C. R. Phys.* **2004**, *5*, 315 – 324; c) P. Bhattacharya, K. Harris, A. P. Lin, M. Mansson, V. A. Norton, W. H. Perman, D. P. Weitekamp, B. D. Ross, *Magn. Reson. Mater. Phys. Biol. Med.* **2005**, *18*, 245 – 256.
[13] a) C. Bianchini, O. Barbaro, *Top. Catal.* **2002**, *19*, 17 – 32; b) D. J. Cole-Hamilton, *Science* **2003**, *299*, 1702 – 1706.
[14] I. V. Koptyug, K. V. Kovtunov, S. R. Burt, M. S. Anwar, C. Hilty, S.-I. Han, A. Pines, R. Z. Sagdeev, *J. Am. Chem. Soc.* DOI: 10.1021/ja0686530.
[15] a) M. S. Anwar, D. Blazina, H. A. Carteret, S. B. Duckett, J. A. Jones, C. M. Kozak, R. J. K. Taylor, *Phys. Rev. Lett.* **2004**, *93*, 040501; b) D. Blazina, S. B. Duckett, C. M. Kozak, R. J. K. Taylor, M. S. Anwar, J. A. Jones, H. A. Carteret, *Magn. Reson. Chem.* **2005**, *43*, 200.
[16] M. S. Anwar, *NMR Quantum Information Processing using Para-Hydrogen*, DPhil Thesis, University of Oxford, **2004**.
[17] a) O. W. Sørensen, G. W. Eich, M. H. Levitt, G. Bodenhausen, R. R. Ernst, *Prog. Nucl. Magn. Reson. Spectrosc.* **1983**, *16*, 163 – 192; b) R. R. Ernst, G. Bodenhausen, A. Wokuan, *Principles of Nuclear Magnetic Resonance in One and Two Dimensions*, Clarendon Press, Oxford, **1987**.
[18] A. Messiah, *Quantum Mechanics*, Dover Publications, USA, **1999**.
[19] S. G. Shyu, S. W. Cheng, D. L. Tzou, *Chem. Commun.* **1999**, 2337 – 2338.
[20] J. M. Brown, P. L. Evan, A. R. Lucy, *J. Chem. Soc. Perkin Trans. 2* **1987**, 1589 – 1596.
[21] a) M. Carravetta, O. G. Johannessen, M. H. Levitt, *Phys. Rev. Lett.* **2004**, *92*, 153003; b) M. Carravetta, M. H. Levitt, *J. Am. Chem. Soc.* **2004**, *126*, 6228 – 6229.
[22] R. Freeman, *Spin Choreography: Basic Steps in High Resolution NMR*, Oxford University Press, Oxford, **1998**.
[23] J. R. MacFall, H. C. Charles, R. D. Black, H. Middleton, J. C. Swartz, B. Saam, B. Driehuys, C. Erickson, W. Happer, G. D. Cates, G. A. Johnson, C. E. Ravin, *Radiology* **1996**, *200*, 553 – 558.

